Indoor Positioning with UWB Beamforming

Christiane Senger[a], Thomas Kaiser[b]

[a]University Duisburg-Essen, Germany, e-mail: c.senger@uni-duisburg.de
[b]University Duisburg-Essen, Germany, e-mail: thomas.kaiser@uni-duisburg.de

Abstract - *Ultra Wideband* **(UWB) is often discussed in connection with localization. A new algorithm called** *BeamLoc* **[1] will be presented in this contribution, which has the capabilities to localize also in NLoS (***Non Line of Sight***) situations. Therefore, no a-priori information about the environment is needed, only a common spatial reference system of the transmitter and the receiver - called** *spatial synchronization***. A beamformer at transmitter and receiver side is applied, which enables one to estimate the direction of the transmitter.**

1 Introduction

Indoor localization is a challenging problem. The huge UWB bandwidth of up to 7.5 GHz allows high resolution, but it also has to deal with a rich multipath environment. The UWB indoor impulse response consists of up to a hundred paths with a delay spread between 10 ns and 30 ns. The impulse response is composed of the direct path and of reflected paths. The *Direct Path* (DP) is the physically existing path going from transmitter (TX) to receiver (RX) without any reflection.

Different scenarios have to be managed (see Figure 1), of which the simplest one is the situation, where the TX can directly see the RX (LoS: *Line of Sight*). The localization in such a LoS situation (Figure 1 left) is solved using ToA (Time of Arrival) estimation [2], which yields a high resolution due to the huge bandwidth in UWB systems. The NLoS environment (Figure 1 middle) is more complicated, since the delay τ of the direct path does not correspond to the distance between TX and RX regarding the simple relationship $d = \tau c$ with c the speed of light. The object (e.g. cupboard, wall) causes an additional delay due to a slower propagation speed inside the object. In an unknown environment, where the properties of the object are unknown, the calculated distance between TX and RX will have a positive biased error. The right scenario in Figure 1 demonstrates a situation where the DP is not necessarily the strongest nor the first arriving path. The additional delay of the DP due to the obstacle can be greater than the relative delay of the reflected path.

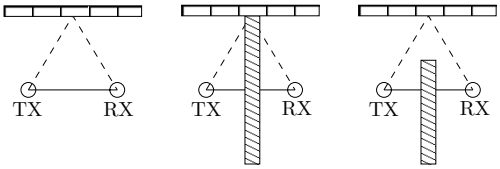

Figure 1: Three Possible Multipath Scenarios. Solid Line: Direct Path, Dashed Line: Reflected Path

The algorithm presented in the following is able to identify the DP under the hundreds of multipaths even when the DP is not the strongest and is not the first path.

2 Mathematical Description

In this section the mathematical signal description will be derived that is used in all further sections.
A directivity behavior on transmitter or receiver side can be achieved by applying an antenna array or a single rotating antenna with a directivity pattern. In this contribution only single rotating antennas will be considered for simplicity. The time-variant beampattern is defined by

$$b(t, \theta, \phi)$$

with the steering direction of the beamformer θ and the direction of the signal ϕ. An integration over time gives a time independent quantity

$$b(\theta, \phi) = \sqrt{\int_{-\infty}^{\infty} b^2(t, \theta, \phi) \mathrm{d}t}.$$

If $s(t)$ is the signal on the transmitter side before the beamformer, the signal after the beamformer is

$$x(t, \theta_T, \phi_T) = b_T(\theta_T, \phi_T) s(t), \tag{1}$$

where the lower index T denotes the transmit side.
The channel, the transmit signal has to pass through consists of several paths k with an amplitude α_k and a delay τ_k

$$h(t) = \sum_{k=1}^{K} \alpha_k \delta(t - \tau_k), \tag{2}$$

(see section 3 for further analysis of the impulse response). The receive signal including a receive beampattern b_R is given by

$$y(t) = \sum_{k=1}^{K} \alpha_k \, b_T(\theta_T, \phi_{T,k}) \, s(t - \tau_k) \, b_R(\theta_R, \phi_{R,k}), \tag{3}$$

where the lower index R marks the receive side. The angles $\phi_{T,k}$ and $\phi_{R,k}$ respectively denote the DoD (*Direction of Departure*) and the DoA (*Direction of Arrival*) of path k.

3 Impulse Response

UWB impulse responses strongly distinguish from narrowband impulse responses. An UWB pulse with a pulse width of 1 ns corresponds to a resolution of 30 cm. Therefore, the UWB impulse response is characterized by numerous resolvable multipaths: in fact, more than 100 multipath components are possible. The typical delay spread is about 10 ns to 30 ns.
In order to be independent of measurement campaigns, a site specific impulse response is derived by using a ray tracing algorithm, which is based on the physically propagation behavior of waves. For simplicity only 2-D scenarios are considered. The reflections are calculated by the mirroring method, where the property given by Snell's law, incident angle equals reflected angle, is exploited. The fact that the refracted angle is different from the incident angle is neglected

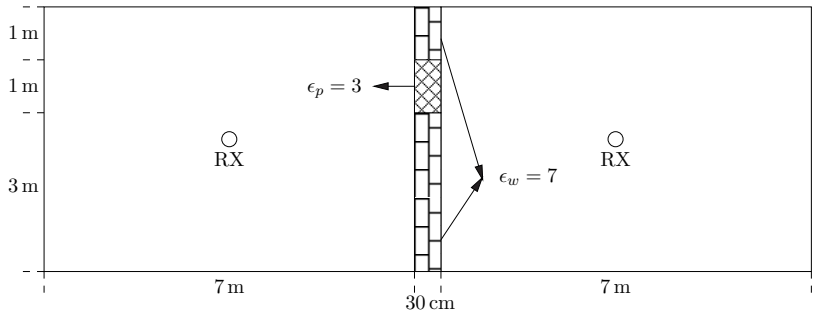

Figure 2: Room Setup: Two rooms 5 m x 7 m separated by a wall with dielectric constant $\epsilon_w = 7$ and a piece with $\epsilon_p = 3$ (e.g. a door).

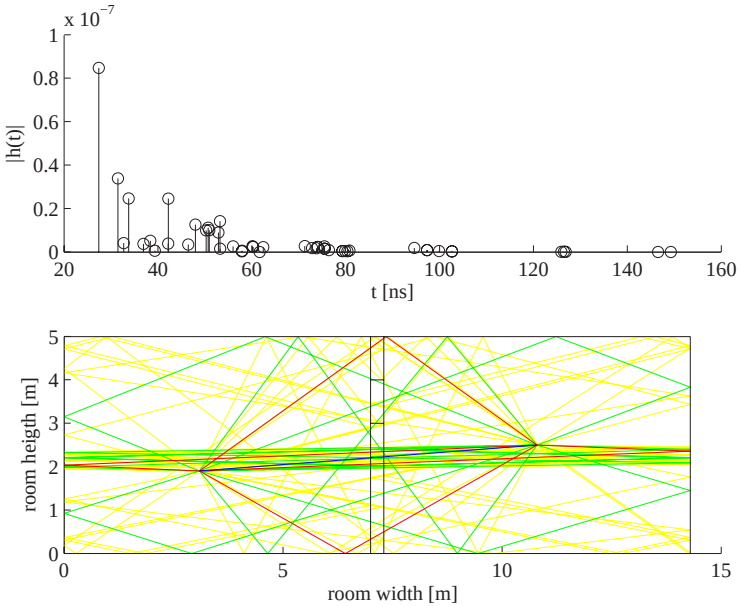

Figure 3: Impulse Response over Time (Upper) and Reflected Paths in Space (Lower)

so far.
Figure 2 shows the chosen room setup. The two rooms are considered with a size of 5 m x 7 m separated by a 30 cm thick wall with two different dielectric constants ϵ_w and ϵ_p. A surrounding dielectric constant of 9 is assumed.
The upper part of Figure 3 gives a sample impulse response for this setup with up to triple reflections, which are shown in the lower part. Included effects are Friis Law, namely the free space propagation loss

$$PL(d) = \left(\frac{c}{f_c 4\pi d}\right)^2$$

where d is the distance in meter and f_c is the center frequency in Hz. Reflection and transmission coefficients are taken into consideration as well as the speed of propagation according to

$$c = \frac{c_0}{\sqrt{\epsilon_r}}$$

with c_0 speed of light and ϵ_r the dielectric constant of the material.
Notice, the number of multipaths in this example is only 52 due to the restriction to 2-D scenarios and also scattering and diffraction effects are not being considered till now.

4 Beamforming

The beamformer consists of an equidistant circular antenna array with N elements, see Figure 4. Note that further indices are omitted since - thanks to antenna reciprocity - the following applies to the transmitter and the receiver as well. A simple beamformer exploits the delays of the signals between the different array elements n

$$\tau_n(\theta, \phi) = (\cos(\gamma_n - \theta) - \cos(\gamma_n - \phi))\,\frac{L}{c},$$

where L is the radius of the circular array and

$$\gamma_n = \frac{n-1}{N} 360^\circ$$

is the angle of antenna element n relative to the array axis. The angles θ and ϕ are the look direction of the beamformer and the DoA of the signal, respectively. The beamformer output is

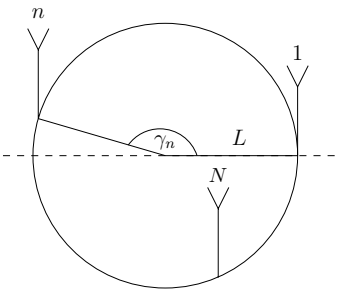

Figure 4: Circular Antenna Array

given by

$$b(t,\theta,\phi) = \sum_{n=1}^{N} x_n(t - \tau_n(\theta,\phi))$$

with $x_n(t)$ the receive signal at antenna n. The beampattern will be defined as

$$b(\theta,\phi) = \max_t \left(\int_{t-T_p/2}^{t+T_p/2} |b(t,\theta,\phi)|^2 \mathrm{d}t \right)^{1/2}, \tag{4}$$

with T_p the length of the transmitted pulse. Figure 5 shows the normalized beampattern for varying array size L and number of antennas N. The center wavelength $\lambda_c = 4.4\,\mathrm{cm}$ is determined by the center frequency $f_c = 6.85\,\mathrm{GHz}$. The received signal is set to the second derivative of the Gaussian pulse

$$p(t) = \left(1 - 2\left(\frac{t}{\tau_p}\right)^2\right) \mathrm{e}^{-\left(\frac{t}{\tau_p}\right)^2}$$

with $\tau_p = 0.0233\,\mathrm{ns}$ scaling the pulse width. Notice, for $N = 2$ antennas the beampattern is unambiguous: it cannot be distinguished if the signal arrives from 90° or 270°. The beampattern becomes ambiguous for more than two antennas independent of the array size. This is a benefit compared to narrowband beamforming, where so called grating lobes occur for $L \geq \frac{\lambda_c}{2}$. The properties of the beampattern are:

1 Mainlobe beamwidth can be decreased by increasing array size or decreasing pulse width.

2 Sidelobe level can be reduced by increasing the number of antennas.

3 Double dB gain for the fixed sidelobe level

More details about UWB beamforming are presented in [3].

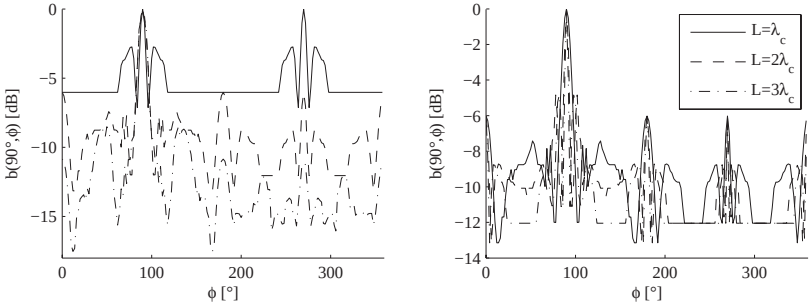

Figure 5: Normalized Beampattern: (left) $L = \lambda_c$, Solid Line: $N = 2$, Dashed Line: $N = 4$, Dashed-Dotted Line $N = 8$, (right) $N = 4$

5 BeamLoc Algorithm

The position of the transmitter, which can have an arbitrary position, should be estimated. The receiver is an Access Point (AP) installed in the center of each room. Figure 6 illustrates the

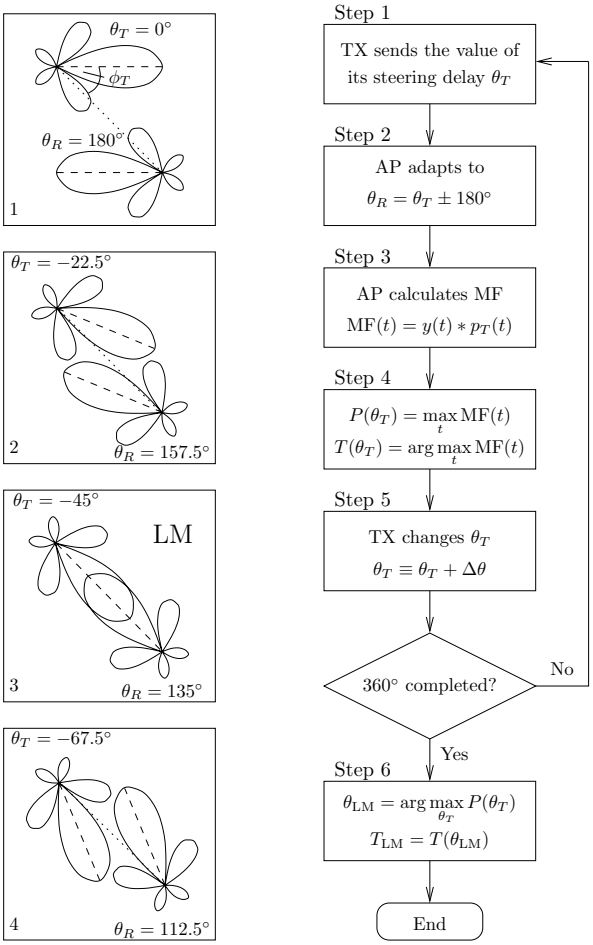

Figure 6: BeamLoc, Left: Principle, No. 3 shows the Locked Mode, Right: Algorithm Flowchart

algorithm and gives the algorithm flowchart. The main idea of the BeamLoc algorithm is to use the fact that the DoD and the DoA of the direct path differ by 180°, i.e.

$$\phi_{T,\mathrm{DP}} = \phi_{R,\mathrm{DP}} + 180^\circ, \tag{5}$$

and estimate the DoA due to this relationship. Hence, the transmitter and the AP need a common spatial reference system, let us call it the *spatial synchronization*. This can be done by equipping the TX and the AP with a compass. The transmitter reports its actual steering direction, θ_T to the AP, which then adapts its steering direction to $\theta_R = \theta_T + 180^\circ$ (Step 1+2). The AP applies a matched filter (MF) to the received signal $y(t)$ with the transmitted pulse shape $p_T(t)$, and afterwards the peak filter output including its time stamp are stored (Step 3+4). Next, the transmitter changes the steering direction by $\Delta\theta$ as long as one rotation is completed (Step 5) and branches to Step 1. In the last step, the *Locked Mode* (LM), the state where TX and AP steer to each other, is detected by evaluating the argument of the maximum received energy. Now, a DoA $\hat{\theta}_{\mathrm{DP}}$ and ToA $\hat{\tau}_{\mathrm{DP}}$ estimate of the direct path are available. If two APs are considered, two DoA and two ToA estimates can be combined in four ways to estimate the position Q of the transmitter, listed in Table 1. The denotation of the resulting estimation error is given in the last column of the table. Also, a weighted averaging over all estimated positions is supposable.

	$\hat{\theta}_{\mathrm{DP},1}$	$\hat{\tau}_{\mathrm{DP},1}$	$\hat{\theta}_{\mathrm{DP},2}$	$\hat{\tau}_{\mathrm{DP},2}$	error
$\hat{Q}_{\mathrm{DoA}}$	x		x		ϵ_{DoA}
$\hat{Q}_1$	x	x			ϵ_1
$\hat{Q}_2$			x	x	ϵ_2
$\hat{Q}_{\mathrm{ToA}}$		x		x	ϵ_{ToA}

Table 1: Possible Combinations of Estimates

6 Simulation Results

The simulation results are based on the scenario given in Figure 2. Fourty TX positions arbitrary located in the left room are chosen. The wall thickness is set to 0.3 meters. We assume that the size of each room is small enough to be covered by one AP, but large enough so that the plane wave assumption is reasonable. Furthermore, both the transmitter and the APs are able to perform beamforming. For all following simulation results, assume $N_T = N_R = N$ and $\lambda_c = 4.4\,\mathrm{cm}$. The impulse response is simulated according to section 3, where the channel is distorted by additive white Gaussian noise. The error is averaged over the 40 TX positions.
The following effects can be observed in Figure 7-10:

- With increasing number of antennas the error decreases. This is due to property 2 of the UWB beampattern. The undesired multipath components (the reflected paths) are better suppressed due to a reduced sidelobe level.
- With decreasing pulse width or increasing array size, the error decreases. This results from property 1 of the beampattern. The direct path can be filtered out better as the mainlobe width is reduced.
- With decreasing step size $\Delta\theta$ the error decreases, which is obvious since a smaller step size entails a higher spatial resolution.

- The combination of ToA and DoA estimate of AP1 is always the best, which is expected, as this is always a LoS situation.
- For high SNR values ϵ_{DoA} outperforms ϵ_2.
- Because of a high ToA error at AP2 the error ϵ_2 is pretty high even for high SNR.
- The combination of ToA and DoA estimate of AP1 is always the best, since this is always a LoS situation.
- For high SNR values ϵ_{DoA} outperforms ϵ_2.
- Because of a high ToA error at AP2 the error ϵ_2 is pretty high even for high SNR.

7 Conclusion

The BeamLoc algorithm was investigated concerning its ability to estimate the DoA of the direct path. In combination with the high temporal resolution of UWB systems, the capability to localize were shown. Further enhancements are considerable as to combine more than two AP results and somehow weight the estimated DoAs and ToAs. An aspect that has to be investigated in more detail is the impact of Snell's law, i.e. the refraction due to transmission. Also, more sophisticated beamformers will be a focus of our future research.

References

[1] Thomas Kaiser, Christiane Senger, Bamrung Tau-Sieskul, and Amr Elthaer, *Localization in Non-Line-Of Sight Scenarios with Ultra-Wideband Antenna Arrays*, Wiley, to appear 2006.

[2] Sinan Gezici, Zhi Tian, Georgios B. Giannakis, Hisashi Kobayashi, Andreas F. Molisch, H. Vincent Poor, and Zafer Sahinoglu, "Localization via ultra-wideband radios," *IEEE Signal Processing Magazine*, 2005.

[3] Sigmar Ries and Thomas Kaiser, "Ultra wideband impulse beamforming: It's a different world," *Special Issue on Signal Processing in UWB Communications*, to appear.

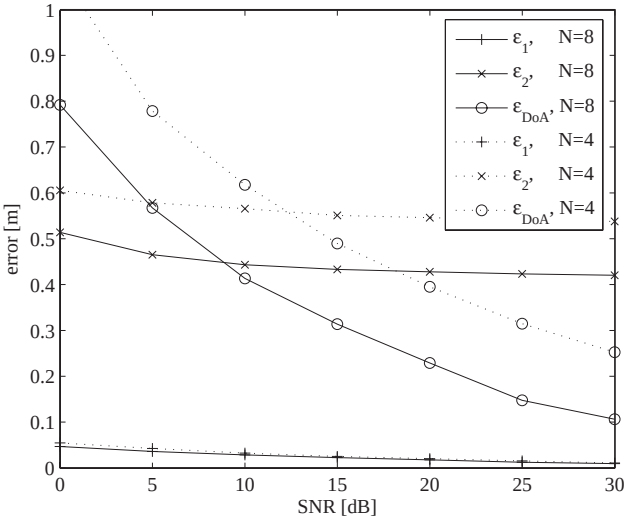

Figure 7: Position Error for $L = \lambda_c$, $T_p = 0.5\,\text{ns}$, $\Delta\theta = 1°$

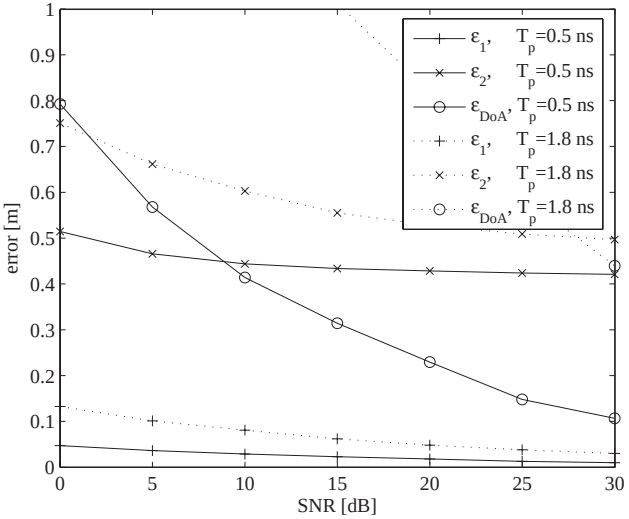

Figure 8: Position Error for $L = \lambda_c$, $\Delta\theta = 1°$, $N = 8$

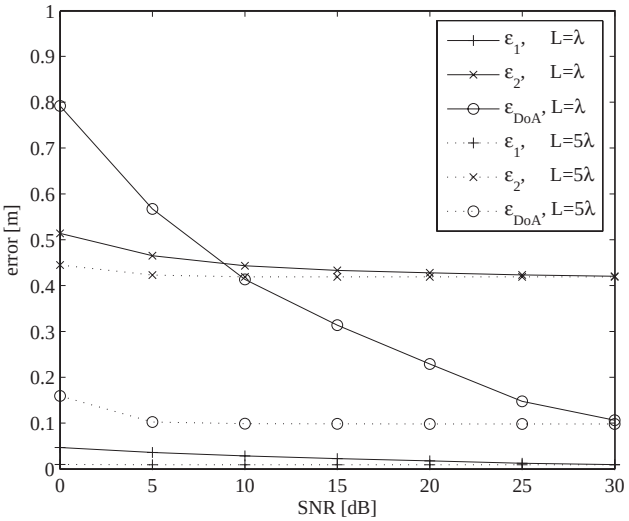

Figure 9: Position Error for $T_p = 0.5\,\text{ns}$, $\Delta\theta = 1°$, $N = 8$

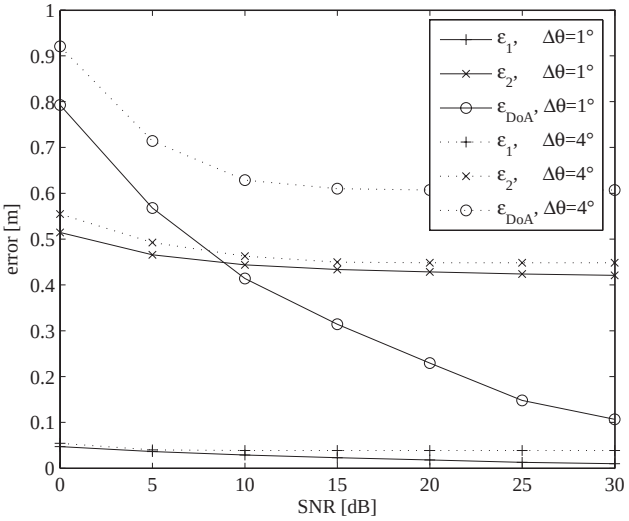

Figure 10: Position Error for $L = \lambda_c$, $T_p = 0.5\,\text{ns}$, $N = 8$